Elastic Deformation of Polycrystals

Rajeev Ahluwalia, Turab Lookman, and Avadh Saxena
Theoretical Division, Los Alamos National Laboratory, Los Alamos, New Mexico, 87545, USA

(Received 17 September 2002; published 28 July 2003)

We propose a framework to model elastic properties of polycrystals by coupling crystal orientational degrees of freedom with elastic strains. Our model encodes crystal symmetries and takes into account explicitly the strain compatibility induced long-range interaction between grains. The coupling of crystal orientation and elastic interactions allows for the rotation of individual grains by an external load. We apply the model to simulate uniaxial tensile loading of a 2D polycrystal within linear elasticity and a system with elastic anharmonicities that describe structural phase transformations. We investigate the constitutive response of the polycrystal and compare it to that of single crystals with crystallographic orientations that form the polycrystal.

DOI: 10.1103/PhysRevLett.91.055501 PACS numbers: 62.20.–x, 61.72.Mm, 81.30.Kf

A study of the mechanical properties of polycrystals is important as most technologically important materials exist in a polycrystalline state. A polycrystal is an aggregate of grains that have different crystallographic orientations. The properties of a polycrystal depend on its texture (distribution of crystallographic orientations). It is desirable to understand how the strains due to an applied external load are distributed and how this influences the average elastic moduli of the polycrystal [1]. An important feature of polycrystals is the evolution of the texture due to rotation of grains during plastic deformation [2]. In the linear elastic regime where plastic effects due to dislocations are not important, there are no significant changes in the orientation distribution on loading. However, for materials that are described by nonlinear elasticity, grain rotations could be important even in the absence of plastic effects. Therefore, a theoretical framework that couples mechanical effects with the orientational degrees of freedom is essential to describe the effective properties of polycrystals.

The problem of finding the effective properties of polycrystals has been studied using averaging techniques [1,3]. However, the complex geometry of a polycrystal or the long-range elastic interactions between the grains are often not accounted for in these methods. In fact, these approaches are only able to give bounds on the effective properties. Recently, the mechanical deformation of polycrystals has been studied by atomistic simulations [4,5] which have been limited to nanosized grains. Simulating bulk systems with atomistic simulations requires enormous computational power and, hence, continuum simulations that can cover a range of intermediate length scales are essential for describing the microstructure at the submicron scale. Several phase-field models have been proposed to model grain growth phenomena [6–8]. Although these models correctly describe the grain morphologies and the domain growth laws, the issues of elasticity and material specific crystal symmetries are usually not addressed. Elastic and plastic effects have been studied with models that describe pattern selection [9]. These are specific only to certain symmetries and do not contain experimentally measured quantities such as elastic constants. In this Letter, we propose a polycrystal model based on continuum elasticity that can be applied to any crystal symmetry and has the appropriate single-crystal elastic constants as input parameters. Elastic strains are coupled to a phase-field model through an orientation field that is determined from a multicomponent order parameter describing the crystal orientations. Because of this coupling, the strains in each grain as well as the grain orientations can change under an external load. This experimentally relevant feature is not accounted for in models that consider static grains created by Voronoi construction [10]. In the present work, we determine the mechanical properties of linear elastic materials and those described by nonlinear elasticity, such as martensites.

The free-energy functional is written as $F = F_{\text{grain}} + F_{\text{elastic}} + F_{\text{load}}$, where F_{grain} is the free-energy density due to the orientational degrees of freedom of the polycrystal, F_{elastic} represents the elastic free energy and F_{load} is the free-energy contribution due to an external applied load. The polycrystalline system is described by a set of Q nonconserved order parameters [6] $(\eta_1, \eta_2, \ldots, \eta_Q)$. A given grain orientation corresponds to one of the Q order parameters being positive nonzero while the rest are zero. The free-energy F_{grain} is given by $F_{\text{grain}} = \int d\vec{r}\{\sum_{i=1}^{Q}[\frac{a_1}{2}\eta_i^2 + \frac{a_2}{3}\eta_i^3 + \frac{a_3}{4}\eta_i^4] + \frac{a_4}{2}\sum_{i=1}^{Q}\sum_{j>i}^{Q}\eta_i^2\eta_j^2 + \sum_{i=1}^{Q}\frac{K}{2}(\nabla\eta_i)^2\}$. For $a_1, a_2 < 0$ and $a_3, a_4 > 0$, the first two terms describe a potential with Q degenerate minima corresponding to Q grain orientations. The gradient energy $(K > 0)$ represents the energy cost of creating a grain boundary. It is also possible to associate an orientational field $\theta(\vec{\eta}, \vec{r})$, where $\theta(\vec{\eta}, \vec{r}) = \frac{\theta_m}{Q-1}[(\sum_{i=1}^{Q} i\eta_i)/(\sum_{i=1}^{Q}\eta_i) - 1]$. Thus, there are Q orientations between 0 and θ_m. For the elastic free energy, the linearized strain tensor in a global reference frame is defined by $\epsilon_{ij} = (u_{i,j} + u_{j,i})/2$ $(i = 1, 2 : j = 1, 2)$, where u_i represents the ith component of the displacement vector and $u_{i,j}$ is its jth displacement gradient. For illustration, we consider a 2D lattice with square symmetry and use the symmetry-adapted linear combinations of the strain tensor defined as [11] $\epsilon_1 = (\epsilon_{xx} + \epsilon_{yy})/\sqrt{2}$, $\epsilon_2 = (\epsilon_{xx} - \epsilon_{yy})/\sqrt{2}$, and $\epsilon_3 = \epsilon_{xy}$. To generalize this theory for the case of a polycrystal, the strain tensor in a rotated frame is calculated as $R[\theta(\vec{\eta})]\epsilon R^T[\theta(\vec{\eta})]$, where $R[\theta(\vec{\eta})]$ is a rotation matrix. Using this transformation, the elastic free energy in a global frame of reference is $F_{\text{elastic}} = \int d\vec{r}\{\frac{A_1}{2}e_1^2 + \frac{A_2}{2}e_2^2 + \frac{A_3}{2}e_3^2 + f_{nl}(e_1, e_2, e_3) + \frac{K_2}{2}(\nabla e_2)^2 + \frac{K_3}{2}(\nabla e_3)^2\}$, where e_1, e_2, and e_3 are defined as $e_1 = \epsilon_1$, $e_2 = \epsilon_2\cos[2\theta(\vec{\eta})] + \sqrt{2}\epsilon_3\sin[2\theta(\vec{\eta})]$, and $e_3 = -(1/\sqrt{2})\epsilon_2\sin[2\theta(\vec{\eta})] + \epsilon_3\cos[2\theta(\vec{\eta})]$. The orientation field $\theta(\vec{\eta})$ is determined from the minima of free energy F_{grain}. Here $A_1 = C_{11} + C_{12}$, $A_2 = C_{11} - C_{12}$, and $A_3 = 4C_{44}$, where C_{11}, C_{12}, and C_{44} are the elastic constants for a crystal with square symmetry. K_2 and K_3 are the appropriate gradient coefficients that in principle can be obtained from experimentally measured phonon dispersion data. The term $f_{nl}(e_1, e_2, e_3)$ represents the nonlinear part of the elastic free energy and is crucial in describing structural phase transitions.

In this Letter, we are interested in simulating a uniaxial loading experiment. If we choose the x axis to be the loading direction, the free-energy contribution due to the external load is $F_{\text{load}} = -\int d\vec{r}\sigma\epsilon_{xx} = -\int dr(\sigma/\sqrt{2})\times(\epsilon_1 + \epsilon_2) = -\int dr(\sigma/\sqrt{2})\{e_1 + e_2\cos[2\theta(\eta)] - \sqrt{2}e_3\times\sin[2\theta(\vec{\eta})]\}$. The strains ϵ_1 , ϵ_2, and ϵ_3 are not independent but satisfy a compatibility relationship [12]: $\nabla^2\epsilon_1 - (\frac{\partial^2}{\partial x^2} - \frac{\partial^2}{\partial y^2})\epsilon_2 - \sqrt{8}\frac{\partial^2}{\partial x\partial y}\epsilon_3 = 0$. Using a method introduced earlier for single-crystal martensitic transformations [13], the strain e_1 may be eliminated using compatibility, to express the effective free energy $F_{\text{eff}} = F_{\text{elastic}} + F_{\text{load}}$ as

$$F_{\text{eff}} = \frac{A_1}{2}\int d\vec{k}|C_2(\vec{k})\Gamma_2(\vec{k}) + C_3(\vec{k})\Gamma_3(\vec{k})|^2 + \int d\vec{r}\bigg[\frac{A_2}{2}e_2^2 + \frac{A_3}{2}e_3^2 + f_{nl}(e_2, e_3) + \frac{K_2}{2}(\nabla e_2)^2 + \frac{K_3}{2}(\nabla e_3)^2 - \frac{\sigma}{\sqrt{2}}\Big(e_2\cos[2\theta(\vec{\eta})] - \sqrt{2}e_3\sin[2\theta(\vec{\eta})]\Big)\bigg],$$

where $\Gamma_2(\vec{k})$, $\Gamma_3(\vec{k})$ represent Fourier transforms of $e_2\cos[2\theta(\vec{\eta})] - \sqrt{2}e_3\sin[2\theta(\vec{\eta})]$ and $e_2(\sin[2\theta(\vec{\eta})]/\sqrt{2}) + e_3\cos[2\theta(\vec{\eta})]$ respectively, $C_2(\vec{k}) = (k_x^2 - k_y^2)/(k_x^2 + k_y^2)$ and $C_3(\vec{k}) = \sqrt{8}k_xk_y/(k_x^2 + k_y^2)$. The long-range terms ensure that compatibility is satisfied within the grains as well as at the grain boundaries.

The dynamics of the grains is given by Q equations $\frac{\partial\eta_i}{\partial t} = -\gamma_\eta\frac{\delta F}{\delta\eta_i}$, where γ_η is a dissipation coefficient and $i = 1, \ldots, Q$ correspond to Q grain orientations. The corresponding overdamped dynamics for the strains is $\frac{\partial e_2}{\partial t} = -\gamma_2\frac{\delta F}{\delta e_2}$, $\frac{\partial e_3}{\partial t} = -\gamma_3\frac{\delta F}{\delta e_3}$, where γ_2 and γ_3 are the appropriate dissipation coefficients for the strains and $F = F_{\text{grain}} + F_{\text{eff}}$ is the total free energy of the system.

The mechanical properties of many materials are well described by the harmonic approximation for which the nonlinear term $f_{nl}(e_1, e_2, e_3) = 0$. For a homogeneous single crystal e_2, e_3, and $\vec{\eta}$ are constant and for Cu $A_1 = 289.8$ GPa, $A_2 = 47.0$ GPa, and $A_3 = 301.6$ GPa ($C_{11} = 168.4$ GPa, $C_{12} = 121.4$ GPa, $C_{44} = 75.4$ GPa). For the parameters in F_{grain}, we choose $a_1 = a_2 = -A_2$, $a_3 = A_2$, $a_4 = 2A_2$, $Q = 5$, and $\theta_m = 45°$. We choose the gradient coefficients in terms of an arbitrary length scale δ so that $K = K_2 = K_3 = A_2\delta^2$ and lengths are scaled by $\vec{r} = \delta\vec{\zeta}$. The free energy F_{grain} then has five degenerate minima defined by $\theta_0(\vec{\eta}) = 0°$, $11.25°$, $22.5°$, $33.75°$, and $45°$, corresponding to five different grain orientations.

To study the polycrystal, we first generate an initial polycrystalline configuration by solving the evolution equations for $\vec{\eta}$, e_2, and e_3 with $\sigma = 0$, using random initial conditions on a 128×128 grid with periodic boundary conditions. For all simulations in this paper, we assume $\gamma_\eta = \gamma_1 = \gamma_2 = \gamma$ and use rescaled time $t^* = t|A_2|\gamma$. For $\sigma = 0$, the elastic effects do not influence the grain growth as all the strains vanish. Grains with orientations $\theta_0(\vec{\eta}) = 0°$, $11.25°$, $22.5°$, $33.75°$, and $45°$ nucleate and coarsen. We arrest the system in a given configuration by suddenly changing the value of the parameter a_1 from $-A_2$ to $-16A_2$. This increases the free-energy barriers between the crystalline states and the growth stops. With the arrested polycrystal configuration as the initial condition, we simulate a quasistatic uniaxial tensile loading using the evolution equations. The stress σ is varied in steps of 0.06 GPa, and we let the strains relax after each change for $t^* = 25$ steps. Figure 1(a) shows the spatial distribution of the polycrystal orientation $\theta_\sigma(\vec{r})$ at a loading of $\sigma = 2.35$ GPa for a system of size $128\delta \times 128\delta$. We note that there is no significant motion of the grain boundaries from the initial arrested configuration to the configuration depicted in Fig. 1(a). The individual grains have rotated by a small amount (max$\sim$0.01°) due to the coupling between stress and the orientation. In Fig. 1(b), we show the corresponding distribution of uni-

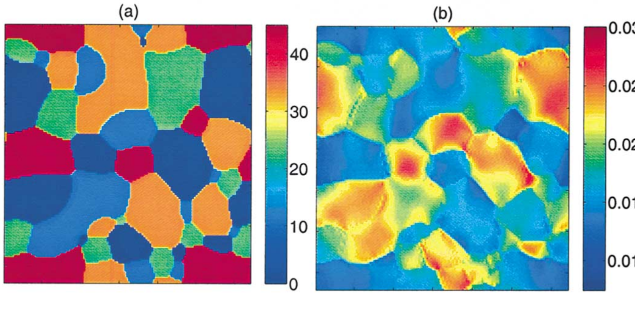

FIG. 1 (color). Spatial distribution of orientation angle $\theta(\vec{r})$ [snapshot (a)] and uniaxial strain $\epsilon_{xx}(\vec{r})$ [snapshot (b)] for stress $\sigma = 2.35$ GPa.

axial strain ϵ_{xx}. It is clear that the strain ϵ_{xx} in a grain depends on the grain orientation.

In Fig. 2 (inset), we show the variation of the average strain $\langle \epsilon_{xx} \rangle$ with the load σ for the polycrystal. For comparison, we also plot the analogous single-crystal curves with crystallographic orientations that constitute the polycrystal configuration in Fig. 1 (single-crystal simulations were performed using only one orientation but with identical free-energy parameters and loading rate as the polycrystal). The Young's modulus of the simulated polycrystal was ~126 GPa. This is in the range of experimentally measured values of 124 GPa [14] and 129.8 GPa [15] quoted for bulk polycrystalline Cu. The result is not sensitive to the choice of parameters for the polycrystal phase-field model, at least in the linear elastic regime.

Another important class of materials that can be studied using this approach are martensites that undergo a displacive structural phase transformation. The transformed phase is characterized by a complex arrangement of crystallographic variants known as twins. We consider the case of a 2D square to rectangle transition for which the deviatoric strain e_2 is the appropriate order parameter. For the high temperature square phase $e_2 = 0$ and for the low temperature martensitic phase $e_2 = \pm e_0$, corresponding to the two rectangular variants. This system exhibits the so-called shape-memory effect which refers to the existence of a *residual* strain on unloading that can be recovered on heating. The microstructure depends on the underlying crystal symmetry and, hence, the displacements and domain wall orientations of the atoms in each grain depend on the grain orientation. Thus, the shape-memory effect will be influenced by the texture and, hence, it is important to compare the mechanical response of single and polycrystal martensites.

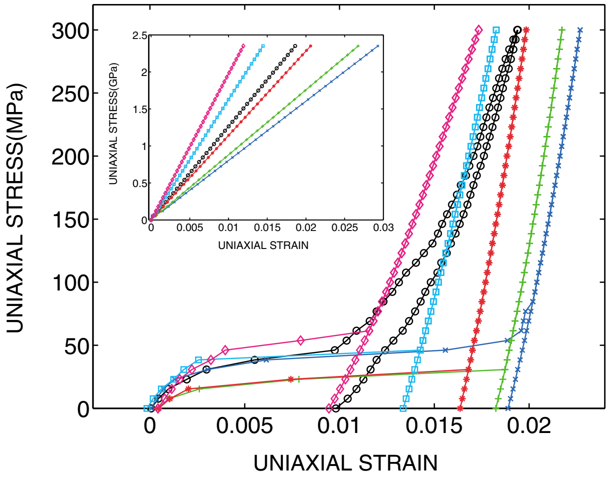

FIG. 2 (color). Average uniaxial strain $\langle \epsilon_{xx} \rangle$ for the martensite as a function of the load σ. The curves correspond to a polycrystal (○) and single crystals with $\theta_0 = 0°$ (×), $\theta_0 = 7.5°$ (+), $\theta_0 = 15°$ (*), $\theta_0 = 22.5°$ (□), and $\theta_0 = 30°$ (◇). (inset) $\langle \epsilon_{xx} \rangle$ vs σ for the linear elastic case. The curves correspond to a polycrystal (black, ○) and single crystals with $\theta_0 = 0°$ (×), $\theta_0 = 11.25°$ (+), $\theta_0 = 22.5°$ (*), $\theta_0 = 33.75°$ (□), and $\theta_0 = 45°$ (◇), from right to left.

The anharmonic contribution to the elastic free energy is given by $f_{nl} = \frac{\alpha}{4} e_2^4 + \frac{\beta}{6} e_2^6$ and describes a first order transition for $\alpha < 0$. We choose $A_1 = 140$ GPa, $A_3 = 280$ GPa, $\alpha = -1.7 \times 10^4$ GPa, and $\beta = 3 \times 10^7$ GPa, parameters that correspond to FePd [16]. The constant A_2 depends on the temperature and we choose $A_2 = -3$ GPa, a temperature in the martensitic phase. The measured gradient coefficient $K_2/a_0^2 = 25$ GPa, where a_0 is the lattice spacing of the crystal and assume $K_3 = 0$ since the deviatoric strain is the dominant mode of deformation. The parameters for F_{grain} are $a_1 = a_2 = -|A_2|$, $a_3 = |A_2|$, and $a_4 = 2|A_2|$, and the grain boundary coefficient is chosen in terms of the lattice spacing a_0 to be $K/a_0^2 = 10^4 |A_2|$. The space variable is rescaled by introducing a dimensionless length scale $\vec{\zeta}$ so that $\vec{r} = (100 a_0)\vec{\zeta}$. The maximum orientation is chosen to be $\theta_m = 30°$ so, for $Q = 5$, the allowed orientations are 0°, 7.5°, 15°, 22.5°, and 30°. With the same procedure as for the linear elastic case, a stable polycrystal configuration is obtained. When the applied stress $\sigma = 0$, the parameter $A_2 = -3$ GPa ensures that the system is well in the martensite phase and domains of the two rectangular variants (twins) are formed. After obtaining a stable martensitic polycrystal, the loading process is simulated by quasistatically varying the stress in steps of 7.6 MPa up to a maximum stress 300 MPa (after each stress change, the system is allowed to relax for $t^* = 25$ steps). The system is then unloaded by decreasing the stress to zero at the same rate.

Figure 3 shows the evolution of variants and the grains at different stress levels during the loading-unloading process for a system of size $12\,800 a_0 \times 12\,800 a_0$. The left column shows the distribution of $\epsilon_2(\vec{r})$ (deviatoric strain in a global frame) and the right column shows the corresponding distribution of the orientations $\theta(\vec{r})$. From Fig. 3 we note that the domain wall orientations depend on the orientation of a grain. On loading, the simulated polycrystal starts to detwin (favored variants grow at the expense of unfavored ones). However, even at the maximum load of $\sigma = 300$ MPa, some unfavorable variants persist. On complete unloading, a domain structure is nucleated again due to inhomogeneities in the polycrystal. However, this domain structure is not the same as that before the loading, indicating an underlying hysteresis. The orientation distribution is also influenced by the external load, as seen in the right column of Fig. 3. The grains with large misorientation with the loading axis rotate significantly (~10°) while the grains with lower orientation do not rotate as much. This is due to the tendency of the system to maximize strain in the loading direction so as to minimize the elastic free energy. At high stress, some grain boundaries start moving to accommodate the applied stress, as seen from the orientation distribution at $\sigma = 300$ MPa.

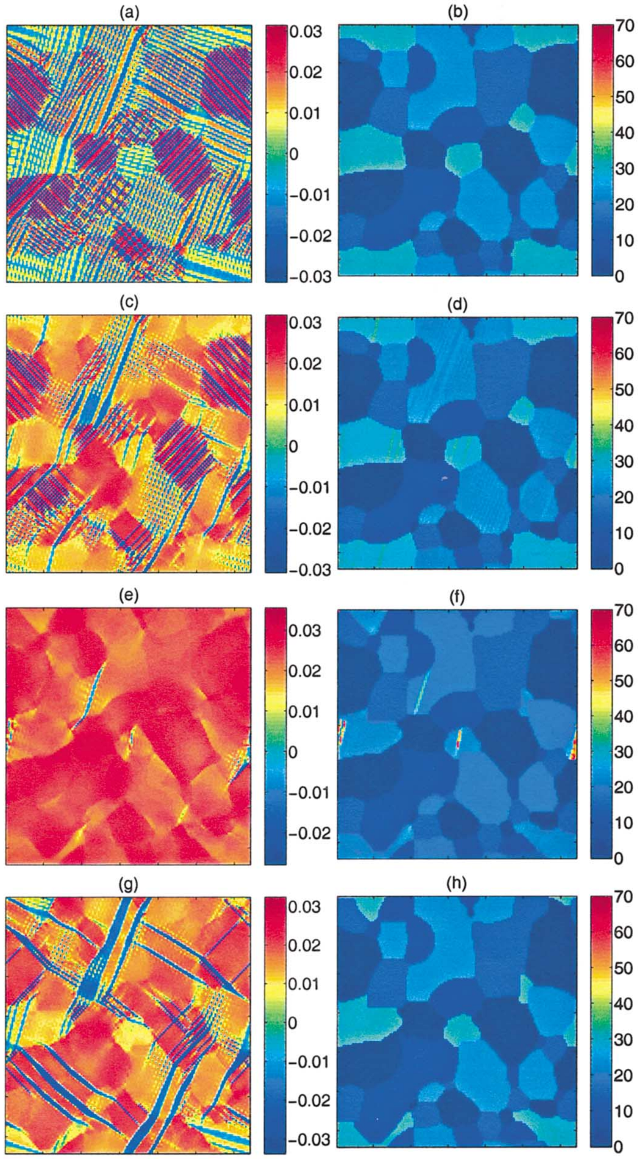

FIG. 3 (color). Spatial distribution of the deviatoric strain in a global frame, $\epsilon_2(\vec{r})$ [snapshots (a), (c), (e), and (g)] and orientation angle $\theta(\vec{r})$ [snapshots (b), (d), (f), and (h)]. The corresponding stress levels are $\sigma = 0$ [(a) and (b)], $\sigma =$ 53.8 MPa [(c) and (d)], $\sigma =$ 300 MPa [(e) and (f)], and $\sigma =$ 0 (after unloading) [(g) and (h)]. The rotations of grains can be inferred from the changing colors of some of the grains. In addition, grain boundary migration occurs at high stresses, as can be seen by comparing (d) and (f).

The stress-strain curve corresponding to Fig. 3 is shown in Fig. 2 (main figure). Also shown are single-crystal curves for all five orientations that constitute the polycrystal of Fig. 3. We observe that the residual strain for the polycrystal case is much smaller than that for a single-crystal oriented along the loading axis. These findings are consistent with the fact that polycrystals have poor shape-memory properties compared to single crystals [3]. The simulations also indicate that grain rotations will influence the mechanical properties of shape-memory alloys. Recently, *in situ* measurements of texture evolution during compression experiments on Ni-Ti shape-memory alloys [17] have been reported. However, these experiments cannot predict whether the changes in texture are due to detwinning or rotation of grains. Our simulations show that both of these processes can contribute to texture evolution.

In summary, we have proposed a framework to study the mechanical properties of polycrystals in which the long-range elastic interaction between grains and the connectivity of the microstructure is taken into account. The approach can be extended to any crystal symmetry or loading (e.g., shear) and does not require any *a priori* assumption of grain shapes or the microstructure. An important feature of our work is the coupling between the grain orientation and elasticity. We have applied the model to study mechanical properties of linear elastic and martensitic materials. For the linear elastic case, the observed grain rotations are small (~0.01°) and, hence, do not influence the mechanical properties. In contrast, the martensitic case shows significant grain rotation (~10°) due to accommodation of the transformation strain. This behavior may be sensitive to the choice of parameters of the polycrystal model (energy barriers between grains) and therefore determination of these parameters from experiment or atomistic simulations will allow accurate prediction of mechanical properties.

We thank Kai Kadau and R. C. Albers for discussions. This work was supported by the U.S. Department of Energy.

[1] M. Avellaneda *et al.*, J. Mech. Phys. Solids **44**, 1179 (1996).
[2] L. Margulies *et al.*, Science **291**, 2392 (2001).
[3] K. Bhattacharya and R.V. Kohn, Arch. Ration. Mech. Anal. **139**, 99 (1997); Y.C. Shu and K. Bhattacharya, Acta Mater. **46**, 5457 (1998).
[4] J. Schiotz *et al.*, Nature (London) **391**, 561 (1998).
[5] H.V. Swygenhoven, Science **296**, 67 (2002).
[6] L. Q. Chen and W. Yang, Phys. Rev. B **50**, 15 752 (1994).
[7] B. Morin *et al.*, Phys. Rev. Lett. **75**, 2156 (1995).
[8] J. A. Warren *et al.*, Physica (Amsterdam) **261A**, 159 (1998).
[9] K. R. Elder *et al.*, Phys. Rev. Lett. **88**, 245701 (2002).
[10] Y. M. Jin *et al.*, Acta Mater. **49**, 2309 (2001).
[11] G. R. Barsch and J. A. Krumhansl, Phys. Rev. Lett. **53**, 1069 (1984).
[12] E. A. H. Love, *A Treatise on the Mathematical Theory of Elasticity* (Dover, New York, 1944).
[13] T. Lookman *et al.*, Phys. Rev. B 67, 024114 (2003).
[14] K. A. Gschneider, Solid State Phys. Adv. Res. Appl. **16**, 275 (1964).
[15] R.W. Hertzberg, *Deformation and Fracture Mechanics of Engineering Materials* (Wiley, New York, 1976).
[16] S. Kartha *et al.*, Phys. Rev. B **52**, 803 (1995).
[17] R. Vaidyanathan *et al.*, Acta Mater. **47**, 3353 (1999).